Estimating instantaneous peak flow from mean daily flow

Bo Chen, Witold F. Krajewski, Fan Liu, Weihua Fang and Zongxue Xu

ABSTRACT

We revisited three traditional methods and proposed a slope-based method, which all require only mean daily flow (MDF) records as inputs, to estimate instantaneous peak flows (IPFs). We applied these methods to 144 basins in Iowa, USA, with drainage areas in the range 7–220,000 km^2. This application involves ~3,800 peak flow events triggered by snow-melting and rainfall over the period from 1997 to 2014. The results show that: using a sequence of MDF rather than just the maximum MDF improves the accuracy of estimating IPFs from MDFs; Sangal's method tends to overestimate, Fill and Steiner's method works reasonably well and is marginally outperformed by the slope-based method. For the slope-based method, about 75% of the basins have prediction error of IPFs within ±10% and about 85% of the basins within ±20%; performances of the four methods degrade as the basin size decreases. Fill and Steiner's and the slope-based methods work well for basins larger than 500 km^2, poorly for basins smaller than 100 km^2, and fairly well for basins with sizes in between. Our proposed method is a simple and promising tool to estimate IPFs from MDFs for areas where IPF records are unavailable or are insufficient.

Key words | flood, instantaneous peak flow, mean daily flow, slope-based method

Bo Chen (corresponding author)
Fan Liu
Weihua Fang
State Key Laboratory of Earth Surface Processes and Resource Ecology,
Beijing Normal University,
Haidian District,
Beijing,
China
E-mail: *bochen@bnu.edu.cn*

Witold F. Krajewski
IIHR-Hydroscience & Engineering,
The University of Iowa,
Iowa City,
Iowa,
USA

Zongxue Xu
Key Laboratory of Water and Sediment Sciences, Ministry of Education,
College of Water Sciences, Beijing Normal University,
Beijing,
China

INTRODUCTION

To avoid underestimation, the use of instantaneous peak flow (IPF) rather than mean daily flow (MDF) is recommended for flood risk management and hydraulic structure design. However, discharge records published are often mean daily values. For data sparse regions, using simple yet effective methods to estimate IPF from MDF deserve more effort. In this paper, we revisit two traditional methods using only sequence of MDF to estimate IPF and propose a new method which is based on the hydrograph shapes of MDF. Additionally, the classical Fuller's method (1914) is used as a reference for accuracy comparison.

For clarity, we summarize the terminology used in related studies. MDF is the average of the river discharge observations for a calendar day, while IPF is the river discharge at the crest of the hydrograph of sub-daily flow. Daily peak flow, used interchangeably with maximum MDF, is the maximum of the MDF recorded over the period (e.g., a few days). The maximum MDF is usually smaller than the associated IPF.

Three groups of methods have been developed in the literature to estimate IPFs from their associated MDFs. The first group regresses the ratio of IPF to the associated maximum MDF (hereafter briefed as peak ratio) against drainage basin characteristics that include but are not limited to drainage area, slope, and length of the longest stream within each basin (e.g., Fuller 1914; Ellis & Gray 1966; Canuti & Moisello 1982). Some works also accounted for the long-term rainfall properties (e.g., Taguas *et al.* 2008). This group of methods generally seeks for the average relationship between the peak ratio and the long-term physiographic and climatic variables, and therefore neglect the within-basin, between-event variability originating from different meteorological inputs. However, floods at the same basin triggered by convective, frontal, and

doi: 10.2166/nh.2017.200

snow-related (e.g., rain-on snow, snow melting) events are found to produce different IPF-MDF relationships (Tan Chiew & Grayson 2007; Taguas *et al.* 2008; Gaál *et al.* 2014), indicating that combining them to obtain a unique IPF-MDF relationship could be problematic. The second group uses hydrologic-modeling (Ding Wallner Müller & Haberlandt 2015), flow disaggregation (Tan *et al.* 2007), and machine-learning based approach (Dastorani *et al.* 2013). With the expense of requiring more data and/or more effort to build models, these methods have the potential to account for the between-event variability of the IPF-MDF relationship originated from short-term controls, such as precipitation and antecedent basin wetness.

The third group of methods specifies IPFs as functions of their associated MDF sequences. These methods assume that, for a storm event, its IPF likely depends on not only the concurrent maximum MDF but also the shape (e.g., the rising and falling speed of the daily discharge hydrograph) of the MDF hydrograph. Langbein (1944) developed the first method of this group, which was later tested for Canadian prairie watersheds by Ellis & Gray (1966). This method is graphics-based and first builds accordance between the shapes of MDF hydrographs and IPFs, i.e., a reference library of the MDF hydrograph shapes and their associated IPFs. Following this, a curve-matching method is used to estimate IPFs from MDFs for the period over which only MDFs are available. Sangal (1983) extended and automated Langbein's method. Sangal's method with constant coefficients was found to tend to overestimate IPFs and was improved by Fill & Steiner (2003) to allow for variable coefficients. Overall, Sangal's and Fill and Steiner's methods are simple and up-to-date approaches that use only MDF sequence to estimate IPF.

Simple, least input-demand yet effective methods to estimate IPFs from MDFs to assist flood risk management are attractive for data-sparse region. Within this context, Sangal's (1983) and Fill & Steiner's (2003) methods have thus far been promising. While Sangal tested his method using 3,946 observed floods at 387 stations of the Ontario streams, about 70% of these stations have drainage areas less than 1,000 km^2 and about 50% of the floods occur during the period of snowmelt. Fill and Steiner applied their method to 117 flood events at 14 stations with drainage area ranging from 84 to 687 km^2. Before recommendation for wider use, the performances of these two methods merit evaluation for basins larger than 1,000 km^2 and for rain-induced floods at more regions. Furthermore, the success of the third group of methods probably originates from their accounting for the shape of hydrographs, i.e., they use the information in the vicinity of the maximum MDF rather than just the maximum MDF. The existing methods that use only MDF records adopt partial means of accounting for hydrograph shapes. For example, some used the ratio of daily peak flow to preceding daily flow and the ratio of daily peak flow to succeeding daily flow (e.g., Langbein 1944; Ellis & Gray 1966), while others used the weighted average of MDFs (Sangal 1983; Fill & Steiner 2003). While the rising and falling slopes, i.e., time derivatives of the discharge $Q(t)$, could be an intuitive and effective alternative to describe the shapes of MDF hydrographs.

The objectives of the present study are twofold. One is to revisit Fuller's, Sangal's and Fill and Steiner's methods, i.e., test their usefulness for wider spatial scales at more basins. The other is to propose an empirical approach, which we call the slope-based method, to estimate IPFs from MDFs. This new method explicitly adopts the rising and falling slopes to describe the shape of a MDF hydrograph. Similar to the two methods to be evaluated, our method is simple and requires only MDF records as its input. Including Fuller's method (1914) as a reference, all these four methods are applied to ~3,800 flood events observed at 144 basins that drain areas ranging from 7 to 221,700 km^2.

The structure of this paper is as follows. First, we introduce Sangal's, Fill and Steiner's, and Fuller's methods and the development of the slope-based method to estimate IPFs from MDFs. We then characterized the study region from the hydrologic point of view and described the runoff data used for this study. The results section presents the application of the four methods at 144 basins in Iowa, USA. We close in the last two sections with a discussion of and conclusion about the usefulness of these methods.

METHODS

All four methods involved in this study consist of two steps. In the first step, peak flow events are selected from the MDF records, and then the methods are used to estimate the associated IPFs. These algorithms take as their inputs the

MDF values preceding and succeeding the day that the maximum MDF occurs and/or the maximum MDF value.

Selection of storm events

We used sub-hourly (one observation every 15 or 30 minutes) discharge data as the primary source of IPFs, which allowed us to assess the performances of the four methods listed in the following sections. We aggregated the continuous sub-hourly series at the 144 basins to daily time series, i.e., the MDF, which were the inputs for the four methods.

Based on the notional peak-over-threshold concept, we identified a total of about 3,800 isolated peak flow events from the MDF records and the 3,800 associated IPFs from the sub-hourly data, i.e. on average, about three events per basin per year. Since our purpose is to study flood flows, we therefore only considered the peak flow events in which the daily peak flow exceeded the threshold, which is the estimate of the 90% quantile of MDF records at each gauge. To make these peak flow events more independent, we required the separation between the daily peak flows of two successive hydrographs from the same basin to be at least 10 days. The threshold and the between-event separation are somewhat subjective, but there is no concrete guidance on how to solve this problem. Tan *et al.* (2007) briefly reviewed this issue and defined their criterion upon it. Our criterion is similar to that used by Tan *et al.* (2007), and we will investigate the influence of the threshold choice on the performances of the four methods. We selected and analyzed these storm events automatically using our in-house R code. While using other criterion to select flood events may partially vary the event sets to be analyzed, it is beyond the scope of this study to investigate this effect.

Fuller's method

Fuller's (1914) method generally uses the following equation to estimate IPF from its associated maximum MDF:

$$Q_{IPF} = Q_{MDF\max}(1 + aA^b) \tag{1}$$

where Q_{IPF} is the instantaneous peak flow in m^3/s, Q_{MDFmax} (m^3/s) is the maximum of the MDF series of a storm event, a and b are regional dependent coefficients and A is drainage area (km^2). In this study, Fuller's method was used as a reference for accuracy comparison, and the values of a and b were determined by regressing the mean peak ratio (Q_{IPF}/Q_{MDFmax}) of each basin against drainage area (144 data points). The values of a (16.96) and b (−0.63) were then used to predicted the IPFs for the 144 basins in our study area. Considering its relative poorer performance and to limit the length of this document, we only present the overall accuracy comparison between Fuller's method and the other three methods.

Sangal's method

Based on examining 3,946 flood hydrographs and assuming a triangular hydrograph, Sangal (1983) proposed the equation

$$Q_{IPF} = \frac{Q_{MDFpre} + Q_{MDFsuc}}{2} + \frac{2Q_{MDF\max} - Q_{MDFsuc} - Q_{MDFpre}}{1 - 2\alpha} \tag{2}$$

where Q_{MDFmax} is the maximum of the MDF series of a storm event, Q_{MDFpre} and Q_{MDFsuc} are MDFs of the day preceding and succeeding the day that Q_{MDFmax} is observed. The term $(1 - 2\alpha)$ is the 'base factor' and it is closely related to the ratio of $(Q_{MDFpre} + Q_{MDFsuc})/2Q_{MDFmax}$. This base factor in practice is important but is unknown and is difficult to determine, therefore, by assuming $\alpha = 0$, Equation (2) was simplified to

$$Q_{IPF} = \frac{4Q_{MDF\max} - Q_{MDFsuc} - Q_{MDFpre}}{2} \tag{3}$$

Note that the coefficients are constant. Equation (3) was applied in the works of Sangal (Sangal 1983), Fill & Steiner (2003) and Dastorani *et al.* (2013). We used Equation (3) in this study.

Fill and Steiner's method

Similar to Sangal's (1983) method, by assuming that the IPF could be estimated as a linear combination of MDFs of three

consecutive days, Fill & Steiner (2003) generalized Equations (2) or (3) to

$$Q_{IPF} = aQ_{MDF\max} + b(Q_{MDFsuc} + Q_{MDFpre}) \quad (4)$$

where a and b are regression coefficients that can be determined over a region using historical data, indicating a and b are constants for a specific region. They further found the necessity to divide Equation (4) by a correction factor

$$Q_{IPF} = \frac{aQ_{MDF\max} + b(Q_{MDFsuc} + Q_{MDFpre})}{0.9123\left[(Q_{MDFsuc} + Q_{MDFpre})/2Q_{MDF\max}\right] + 0.3620} \quad (5)$$

Interestingly, the correction factor, i.e., the denominator in Equation (5), also contains the ratio $(Q_{MDFpre} + Q_{MDFsuc})/2Q_{MDFmax}$ that is important for the 'base factor' of Sangal's method (Equation (2)). From this viewpoint, Fill and Steiner's method allows for adjusting the weights of MDFs of the three consecutive days and ultimately specifies a nonlinear relationship between IPFs and MDFs. Fill & Steiner (2003) and Dastorani *et al.* (2013) set the values of a and b to 0.80 and 0.25, respectively. Similarly, we adopted these values and Equation (5) in our study. The values of a and b are not localized because our goal is to test the usefulness of these methods when only MDF series is available and IPF record is absent.

The slope-based method

This section presents the details of the slope-based method we propose. IPF generally occurs a few hours after the beginning of the day that the maximum MDF occurs (Figure 1) and is apparently larger than the associated maximum MDF. The slope-based method extrapolates the straight line that is determined by the points (t, Q_{MDFpre}) and ($t+1$, Q_{MDFmax}) by r into the day that the maximum MDF occurs, i.e., it extends the line segment from $(t+1)$ to $(t+1+r)$. The vertical ordinate corresponding to $(t+1+r)$ is assumed to be the estimated IPF (see Equation (6) below and Figure 1).

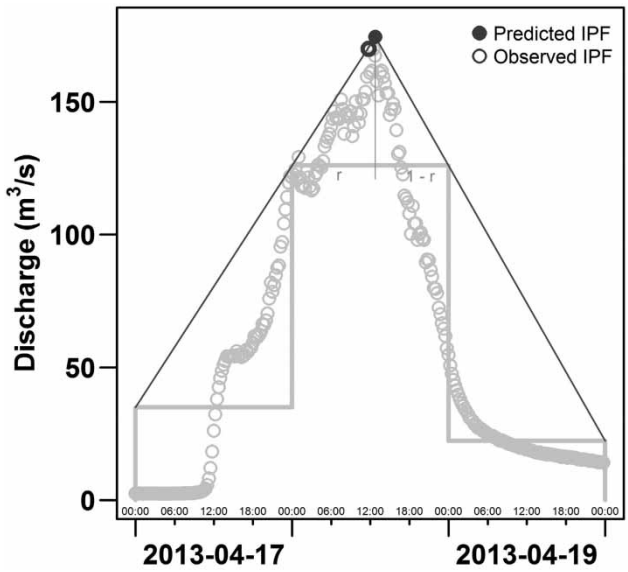

Figure 1 | Illustration of the slope-based method to estimate IPF from MDF. The observed sub-hourly (15-minute) flows are represented as open circles, and the MDFs are plotted as bars. These observations were extracted from the discharge record of the USGS gauge 05454220, which is within the Clear Creek Experimental Watershed Well instrumented by the University of Iowa.

Note that r is bounded by 0 and 1. We assume that the intersection that is determined by extending the rising and falling limbs of a MDF hydrograph towards the hydrograph peak is the associated IPF (Figure 1). This can be mathematically expressed as

$$Q_{MDFpre} + k_r(1+r) = Q_{MDFsuc} + k_f(1+1-r) \quad (6)$$

where k_r is the rising slope of the discharge hydrograph and is estimated as

$$k_r = \frac{Q_{MDF\max} - Q_{MDFpre}}{dt} \quad (7)$$

and k_f is the falling slope and is approximated as

$$k_f = \frac{Q_{MDF\max} - Q_{MDFsuc}}{dt} \quad (8)$$

where $dt = 1$ day in this context. Substituting Equations (7) and (8) into (6) yields

$$r = \frac{Q_{MDF\max} - Q_{MDFsuc}}{2Q_{MDF\max} - Q_{MDFsuc} - Q_{MDFpre}} \quad (9)$$

Consequently, r is determined and can be substituted into Equation (6) to obtain

$$Q_{IPF} = Q_{MDF\max} + \frac{(Q_{MDF\max} - Q_{MDFpre})(Q_{MDF\max} - Q_{MDFsuc})}{2Q_{MDF\max} - Q_{MDFpre} - Q_{MDFsuc}} \quad (10)$$

Performance comparison metrics

Each criterion may have an emphasis on different aspects of simulated and observed behaviors, and thus selecting and interpreting performance efficiency criteria can be a challenge even for experienced hydrologists. For example, applications of the Nash-Sutcliffe and root-mean-square error (RMSE) metrics in the hydrologic community have been criticized by a few works (Legates & McCabe 1999; Krause Boyle & Bäse 2005; Willmott & Matsuura 2005; Willmott & Matsuura 2006; Schaefli & Gupta 2007; Criss & Winston 2008; Piñeiro *et al.* 2008). We decided to follow the suggestion of using multiple approaches (Legates & McCabe 1999) to evaluate the effectiveness of the methods used to estimate IPF.

We used linear regression statistics, mean absolute error (MAE) and mean absolute percentage error (MAPE) to compare the performances of the four methods listed above. These metrics were calculated based on comparing the predicted IPFs against the observed IPFs for each basin. For linear regression statistics our concern is about whether the slope is close to unity and the intercept is not statistically different from 0. MAE, as a measure of prediction error in the original unit of streamflow, is calculated as

$$MAE = \frac{1}{n}\sum_{i=1}^{n} \left|Q_{IPFobs}(i) - Q_{IPFpred}(i)\right| \quad (11)$$

where $Q_{IPFobs}(i)$ and $Q_{IPFpred}(i)$ are the i^{th} observed and predicted IPFs, and n is the number of peak flow events for a basin. MAPE is a relative error measure (has no unit) quantified as

$$MAPE = \frac{1}{n}\sum_{i=1}^{n} \left|\frac{Q_{IPFobs}(i) - Q_{IPFpred}(i)}{Q_{IPFobs}(i)}\right| \times 100\% \quad (12)$$

STUDY AREA AND DATA

The flood generation process is rich in Iowa, USA – the study area of this work – due to the interplay between meteorological inputs and basin characteristics. Iowa has an overall flat terrain and 92% of its territory is occupied by agricultural land. Approximately 75% of the 900 mm average annual precipitation and 85% of the 45–65 thunderstorms over the study region occur from April through September. Frozen soils near the surface last from late October to early April. Flooding has been quite frequent in Iowa in the past three decades, including the extreme widespread events in 1993 and 2008, providing us a good data set to support this study. Floods in Iowa can be generated from snow-melting, frontal, and convective events. Annual maximum streamflows occur typically during the period from April to July. In order to account for the regional differences in flood hydrology (Eash Barnes & Veilleux 2013), flood frequency analysts in Iowa often partition Iowa into eight flood regions (Figure 2) according to its landforms (Prior 1991), topography, geology, and soil. The frequent and multiple generation mechanisms of floods in Iowa provide a good data set to test the IPF estimation methods across wide spatial scales.

We used the sub-hourly discharge records that are available at the USGS IDA website for 144 out of about 180 USGS stream gauged basins located in the State of Iowa. Snow-related events are also included in this study. As shown in Figure 2, these gauges are located in nine different hydrologic regions that are defined by the USGS. Most of these gauges have only minor or no regulations directly upstream. The water levels were automatically recorded and were translated into discharge via the rating curve approach. While the record lengths are longer, we could only access the data from 2007 to 2014 due to database maintenance activities of the USGS data center. The 144 basins drain areas ranging from 7 to 221,700 km^2 and their size distribution are shown in Figure 3. About 70% of the basins are within the 100 to 10,000 km^2 size range, and 10% are smaller than 100 km^2.

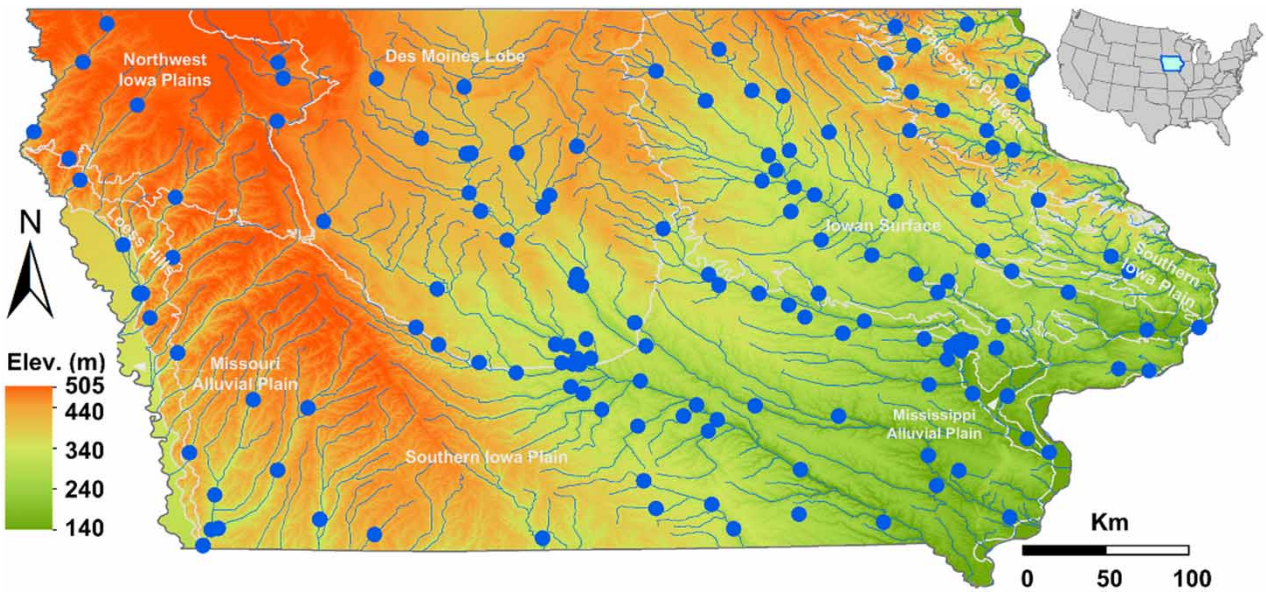

Figure 2 | Topography of Iowa (the highlighted area of the US map in the top-right corner) and the locations of eight flood regions and 144 stream gauges used in this study.

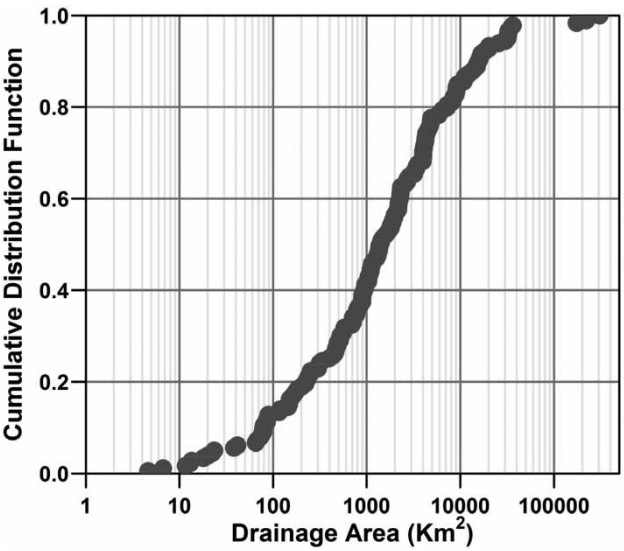

Figure 3 | Cumulative distribution of the sizes of basins used in this study.

RESULTS

Characteristics of the peak flow events used

This study involves a total of 3,822 peak flow events. Out of these, 685 events, accounting for 18% of the total, are observed over the period from January 1 to April 15. Since winter starts in November and snowmelt ends by approximately April 15 for the study region, we assume that these 685 events (of which 485 are in February and March) are snow-related. The IPF hydrographs of these events are generally smoother when compared to the other hydrographs at each gauge. When screening the seasons of peak flow events, we found that snow-related events were more frequent at small basins and rare at large basins (not shown here). The remaining 3,137 events, i.e., 82% of the peak flow events analyzed in this study, are rainfall triggered.

All of the four methods investigated in this study assume that the maximum MDF and the IPF occur on the same day. Analyses show that 3,130 of the 3,822 (82%) IPFs occurred on the same day as the maximum MDF, indicating the assumption is rational. About 15% and 2% of the IPFs occurred on the preceding and succeeding days of the MDF, respectively. Less than 1% of the IPFs occurred two days away from the day that MDF occurred. Most of the nonconcurrent events have IPFs occurring after 19:00.

Figure 4(a) plots the average peak ratio of each basin (represented by the dots) against its drainage area and suggests three notable features. Firstly, though with large scatter, the average peak ratio tends to decrease as the

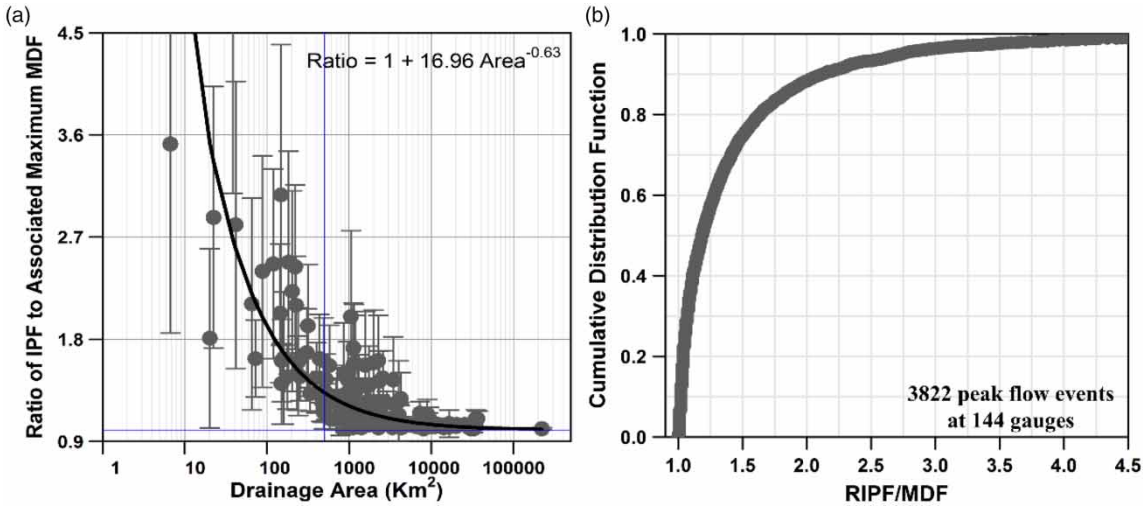

Figure 4 | Characteristics of the peak flow events studied: (a) peak ratio against basin size and (b) cumulative distribution of peak ratios of the peak flow events used in this study. In Figure 4(a), the gray dots are the averages, the bars are the 1 standard deviations of the peak ratios of each basin, the horizontal blue line represents a ratio of 1.0 and the blue line marks a drainage area of 500 km^2, and the equation in the upper-right corner is determined using the gray data points. Please refer to the online version of this paper to see this figure in color: http://dx.doi.org/10.2166/nh.2017.200.

basin size increased, indicating the hydrographs of smaller basins tend to be spikier. Also, especially for smaller basins, the peak ratios for different storms have a wide spread (error bars in Figure 4(a) represent one standard deviation), showing the notable at-a-station between-event variability of the IPF-MDF relationship. Furthermore, the peak ratio tends to asymptote to unity for basins larger than 10,000 km^2 and the at-a-station variability of peak ratios become much smaller for basins larger than 500 km^2. Figure 4(b) shows that about 55% and 90% of events investigated in this study have their peak ratios lying within the intervals of [1.0, 1.25] and [1.0, 2.0], respectively.

Comparison of the observed and predicted IPFs at nine basins

To check the performances of the four methods, we plotted the predicted IPFs using these methods against the observed IPFs for all the 144 basins. We only show the scatterplots of nine basins to limit the length of this document. These basins were selected as representations of basins with different sizes. The performances at all 144 basins will be presented statistically in the next section.

Their application at nine basins in Iowa suggests that the four methods are useful in estimating IPFs from MDFs. Figure 5 compares the predicted and observed IPFs for nine basins through simple linear regression. For basins larger than 150 km^2, the points in the scatter plots are generally located along the 1:1 lines, indicating a regression slope close to unity and an intercept statistically not different from zero. The small spread along the 1:1 line implies a good agreement between the observed and predicted IPFs, as evidenced by the fact that the coefficients of determination (R^2) are greater than 0.91. The keys at the lower-right corners are the regression statistics of predicted IPFs by the slope-based method against the observed IPFs. Fuller's method tends to underestimate IPFs. The other three methods generally give similar IPF estimates, while Sangal's method tends toward overestimation (especially for large flow events) and the slope-based method appears to have the smallest scatter around the 1:1 lines for basins larger than 150 km^2. Figure 5 shows that the performances of the four methods are better for large basins and less effective for small basins (see the first two panels in Figure 5). We will elaborate this shortly in the Discussion section.

Comparison of the observed and predicted IPFs at all basins

The basin-by-basin comparison described above shows the apparent usefulness of the four methods to estimate IPFs

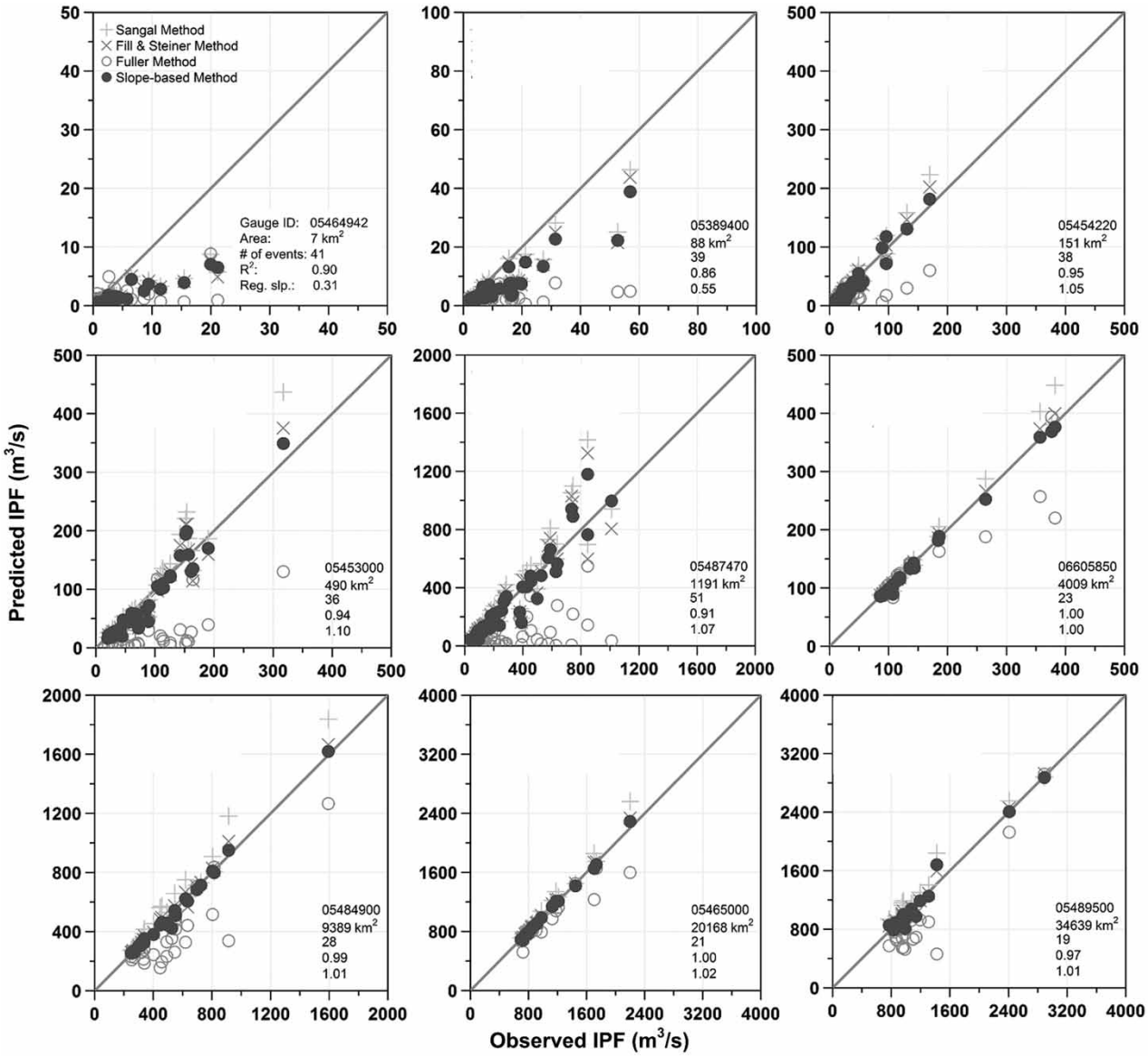

Figure 5 | Simple linear regression-based comparison of the predicted and observed IPFs for nine basins. The 1:1 line is superimposed onto each scatter plot. The last two rows of the keys at the lower right corners of each panel are the results of the slope-based method.

from MDFs at nine basins. To examine whether their skills hold across all of the basins in Iowa, we followed the same procedure to conduct the comparison analyses for the remaining 135 basins.

We focused primarily on comparing the coefficient of determination (R^2), the slope, and the intercept of the simple linear regression of the predicted IPFs against the observed IPFs at each basin. For brevity, we only present the regression statistics of the slope-based method. The coefficients of determination at 127 out of 144 basins investigated in this study are above 0.90, indicating that the majority of the variation in the observed IPFs can be explained by the predicted IPFs. The results show that the regression slopes are statistically significant at a confidence level of 95% for all basins. Since underestimation/overestimation, reflected by the slope of the simple linear regression, is of primary importance for safety design, we will closely examine the values of the regression slope in

the next paragraph. Lastly, we need to determine whether the IPF predictions are biased on average. We rejected the intercepts of the simple linear regression at 138 out of the 144 basins because they were not statistically different from zero at a significance level of 95% (i.e., $p = 0.05$). This means there is a zero intercept (i.e., no bias on average) for the simple regression for most of the basins, which is favorable. Therefore, no intercepts were shown in Figure 5.

It can be observed from Figure 6 that Fuller's method appears to underestimate, Sangal's method tends to overestimate, Fill and Steiner's method shows good performance and the slope-based method appears to marginally outperform Fill and Steiner's method. The first row of Figure 6 illustrates the cumulative distributions of the regression slope of the predicted IPFs against the observed IPFs. Figure 6(a) shows that the regression slopes for 50% of the 144 basins are greater than 1.1, indicating notable overestimation of Sangal's method. Figure 6(b) displays that, for Fill and Steiner's method, about 70% of the basins have regression slopes between 0.90 and 1.10 (i.e., ±10% prediction error in IPFs), and about 85% of the basins have regression slopes between 0.80 and 1.20 (i.e., ±20% prediction error in IPFs). Figure 6(c) illustrates that, for the slope-based method, about 75% of the basins have regression slopes between 0.90 and 1.10, and about 85% of the basins have regression slopes between 0.80 and 1.15. Figure 6(d) shows that, for Fuller's method, about 18% of the basins have regression slopes between 0.90 and 1.10, and the regression slopes for 80% of the 144 basins are less than 0.90 (i.e., notable underestimation of IPFs). Also, the upper limits of overestimation for the slope-based, Fill and Steiner's, Fuller's and Sangal's methods are 15%, 25%, 30% and 40% (maximum regression slopes of 1.15, 1.20, 1.30, and 1.40), respectively.

The second row of Figure 6 displays MAE and MAPE as a function of basin sizes for the four methods. Figure 6(e)

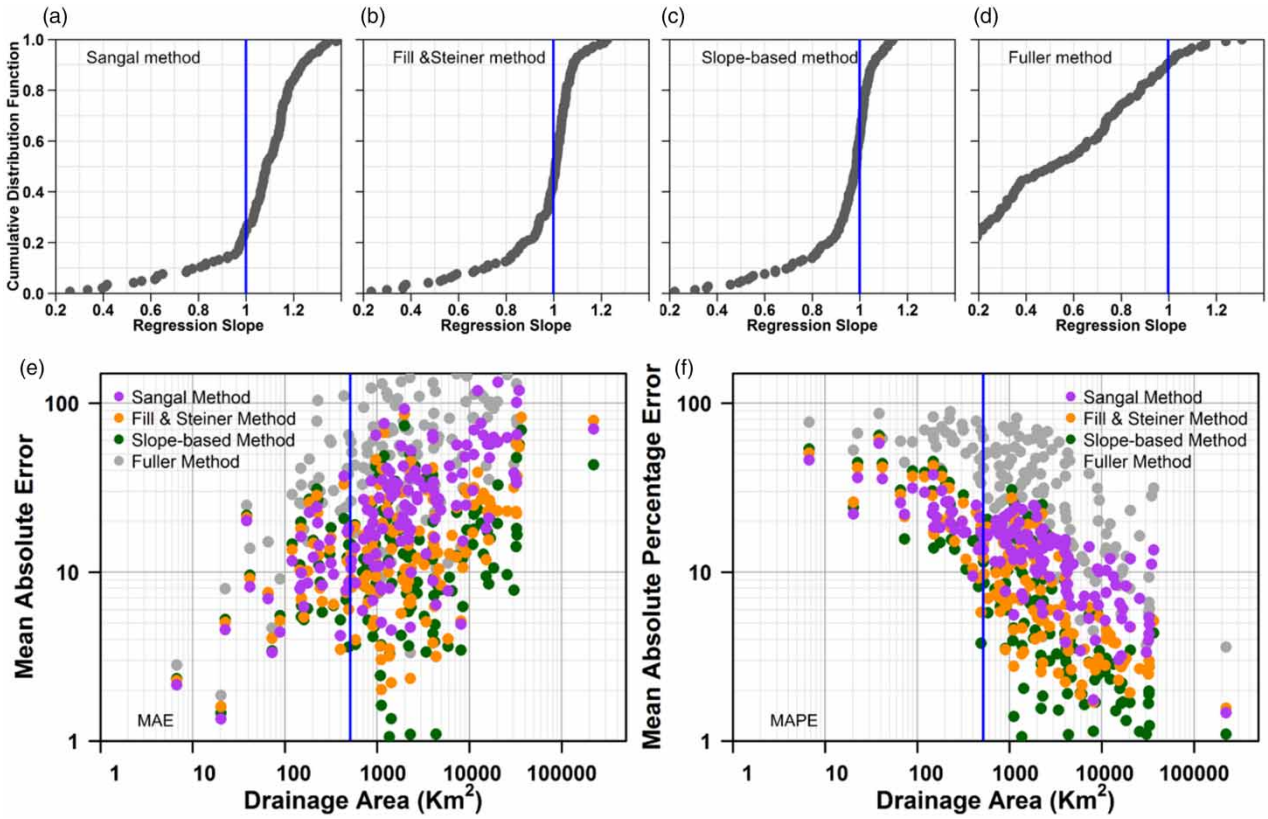

Figure 6 | Performance comparison of the four methods: cumulative distributions of the regression slope of the predicted IPFs by (a) Sangal's, (b) Fill and Steiner's, (c) the slope-based and (d) Fuller's methods against the associated observed IPFs; (e) MAE and (f) MAPE against drainage areas of the 144 basins studied. The blue lines in (e) and (f) represent drainage area of 500 km^2. Please refer to the online version of this paper to see this figure in color: http://dx.doi.org/10.2166/nh.2017.200.

shows that the MAE increases with basin size and Figure 6(f) suggests that the MAPE decreases with basin size. The absolute relative errors are larger for larger basins, while they are relatively small when compared to the flow magnitudes, indicating better prediction performances of the four methods for larger basins. Interestingly, for basins larger than 500 km^2, it seems that the points in Figure 6(e) and 6(f) are layered: the gray points (Fuller's method) on the top most layer, the purple points (Sangal's method) on the second layer, the greens (the slope-based method) at the bottom and the oranges (Fill and Steiner's method) in-between. This means that overall both in the absolute and relative senses, Fuller's method has the largest and the slope-based method has the smallest prediction errors for larger basins. The pattern is reversed for basins smaller than 500 km^2, suggesting that Sangal's method performs best for smaller basins. Due to its overall relative poorer performance, the results of Fuller's method will not be presented in the remaining sections.

Performances for snow-related and rain-related events

Results show that, for snow-related peak flow events, all three methods (Fuller's method not included) tend to estimate IPF well from MDF; while for rain-related events, Sangal's method overestimates and Fill and Steiner's and the slope-based methods perform well. Figure 7(a1) and 7(a2) show that, for Sangal's method, the distributions of the regression slope for snow- and rain-related events center to the right of unity, indicating overestimation of IPFs. The overestimation problem for snow-related events is acceptable but that for rain-related events is considerable. This means that the performance of Sangal's method depends on the peak flow generation mechanism. Recall that Sangal's method was developed based on a data set where 50% of the peak flow events occur during the period of snowmelt, this may explain why it performs better for snow-related events used in this study. For Fill and Steiner's and the slope-based methods (Figure 7(b1, b2, c1, c2)), the distributions of the regression slope for both types of events center at ~1.0, suggesting these methods perform well with wider applicability. Obviously, regardless of the types of peak flow events, all three methods underestimate IPFs for about 15–20% of the basins (usually those small ones) used in this study.

Changing the threshold values from the 90% to the 95% and to the 99% percentiles of the MDFs at each basin to define peak flow events only reduced the total number of peak flow events from about 3,800 to 3,300 and to 2,400 events, respectively, but did not change the above presented prediction performances.

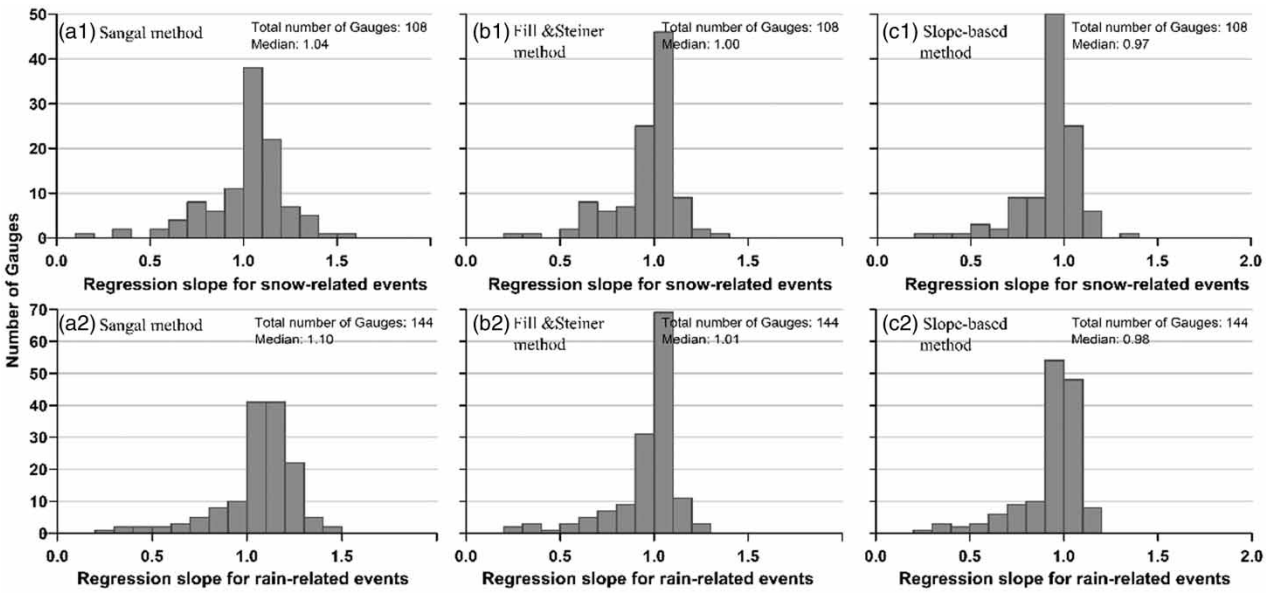

Figure 7 | Performances of Sangal's (a1 and a2), Fill and Steiner's (b1 and b2) and the slope-based (c1 and c2) methods for snow- (upper row) and rain- (lower row) related events.

DISCUSSION

On the relationship between IPF and MDF

These results show that the peak ratio of IPF to MDF generally decreases with an increase in basin size (Figure 4(a)). This cross-station trend is consistent with the conclusion drawn in current literature that basin characteristics have a bearing on the IPF-MDF relationship (e.g., Fuller 1914; Ellis & Gray 1966; Canuti & Moisello 1982; Gupta *et al.* 2010). While the large scatter around the average relationship between IPF and MDF in Figure 4(a), which we called at-a-station variability of peak ratios, signifies other contributing factors to the dependence of IPF on MDF. This notable at-a-station variability probably originates from the climatic forcings or initial conditions of basins prior to peak flow events. For an example, when eye-screening the peak flow events, we found that both snow- and rain-related peak flow events can be found for smaller basins (<500 km^2) while snow-related peak flow events are rare for larger basins (>3,000 km^2). Furthermore, IPFs of similar magnitude but from hydrographs with substantially different shapes can originate from snow-related and rainfall events in the same basin. We also found that even if both originate from rainfall events (events occurring during summer time), two similar IPFs can be extracted from hydrographs with notable shape discrepancy. Blending these peak flow events that have different runoff generation processes at least partially leads to the more variable IPF ratios at smaller basins. This at-a-station variability supports the argument that floods generated from different meteorological inputs normally produce hydrographs of different shapes (Figure 7) and, thus, different IPF-MDF relations (e.g., Ellis & Gray 1966; Taguas *et al.* 2008; Gaál *et al.* 2014). Other factors, for examples, the lengths, altitudes, soil thickness and mean annual precipitation may also affect the IPF-MDF relationship (Canuti & Moisello 1982; Taguas *et al.* 2008; Serinaldi & Kilsby 2013). Regarding the cross-station trend, generally, large basins tend to have high flows over at least a day with relatively slow rising and falling speeds while small basins have flood hydrographs over a few hours with rapid rises and recessions. This explains why the smaller the basin, the spikier the hydrographs and the larger the peak ratios, and vice versa. With respect to the at-a-station variability, hydrographs generated from snow-melting, frontal rains and convective rains have increasing spikiness (Gaál *et al.* 2014) and therefore increasing peak ratios. The spikier the hydrograph, the less similar the shapes between hydrographs of IPF and MDF. The cross-station decreasing trend and the at-a-station remarkable variability collectively suggest that the IPF-MDF relationship depends on the interaction between the basin characteristics and the climatic forcings.

Incorporating hydrograph shape information to estimate IPF

The application of the four methods in Iowa, a region with different flood hydrology in space and time, suggests that accounting for the dynamics of MDF hydrograph shapes is an effective approach to estimate IPFs from MDFs (Figures 5 and 6). Fuller's (1914) method uses only the maximum MDF from a hydrograph to estimate the associated IPF, i.e., only limited information from the hydrograph has been used, and this resulted in its relatively poorer performance. In contrast, Sangal's (1983) method uses the three-day consecutive MDF sequence, while the weights are kept constant in practice or are difficult to adjust for each peak flow event (Equation (2)). This leads to reduced but still relatively large estimation errors and the problem of overestimating IPFs for large basins (Figure 6). Inspired by Sangal (1983), Fill & Steiner's (2003) method and the slope-based method proposed in this study add correction factors that are designed to consider the dynamic hydrograph shapes of each individual peak flow events. Their good performances across vast spatial scales (7 to 220,000 km^2), various flood regions and 3,800 peak flow events triggered by different precipitation configurations in Iowa suggest that Fill and Steiner's method and the slope-based method tend to be robust and useful. The sloped-based method showed marginal improvement to Fill and Steiner's method, and it is conceptually similar to other approaches (Jarvis 1936; Sangal 1983; Fill & Steiner 2003; Tan *et al.* 2007), but it explicitly uses the rising and falling slopes to characterize the shape of MDF hydrographs. These observations would be expected as we discussed in the previous section – the

shape of the hydrograph, rather than just the hydrograph peak, is a comprehensive indicator of the interplay between meteorological inputs and basin characteristics. This finding is consistent with that of Tan *et al.* (2007), though they adopted a different strategy. Therefore, when estimating IPFs from MDFs, it would be helpful to use not only the maximum MDF but also the MDF values in the vicinity of (i.e., 1–3 days before and after) the day that the maximum MDF occurs. Overall, Fill & Steiner's (2003) method and the slope-based method have the potential to be applied in other regions, though further tests are recommended if it is feasible. However, the degree of shape similarity between daily and instantaneous hydrographs determines the upper limits of how successful one can estimate IPFs from MDFs (Tan *et al.* 2007). The spikier the IPF hydrographs, the less similar the shapes of the IPF hydrographs and their associated MDF hydrographs are, and vice versa.

The limitations of estimating IPF from MDF

All the four methods using MDFs to estimate IPFs share some common limitations, many of which stem from the fact that only information with coarse temporal resolution (MDFs) is available (Figures 8 and 9). They tend to have reasonable prediction accuracy for basins larger than 500 km^2. For example, Figure 8(c) shows that, for the majority of the basins larger than 500 km^2, the regression slopes of predicted IPFs against observed IPFs are within the range of [0.75, 1.15], indicating good performance of the slope-based method, while the regression slopes spread over the ranges of [0.50, 1.10] for basins with sizes between 100 and 500 km^2 and [0.22, 0.65] for basins smaller than 100 km^2.

Underestimation is prevalent for basins smaller than 500 km^2, which can be caused by several factors. One is that the hydrographs of smaller basins tend to be spikier, i.e., smaller basins tend to have higher IPF-MDF ratios (Figure 4(a)). Another factor is that hydrographs with higher observational frequencies are double-peaked, but this feature is not visible from the hydrograph of MDFs (Figure 9(b)). A third factor is that the abnormally sharp rising limb of an hourly hydrograph is not reflected in the MDF hydrographs (Figure 9(c)). For the event represented by the circled dot in Figure 9(c), the hourly hydrograph has an extremely sharp rising limb, which is six times that of the normal rising speed at this basin. Furthermore, all four methods have a hidden assumption that maximum MDF and IPF occur on the same day, which have 18% chance to be invalid in our study area. This non-concurrence may lead to underestimation of IPFs as exemplified in Figure 9(d). Each of the last three scenarios produces one bad prediction that noticeably lowers the regression slope. Accordingly, we flag these basins as overall underestimation. These problems become increasingly insignificant as the basin size increases because flow conditions vary more slowly for larger basins, and, thus, more information about IPFs can be retrieved from MDF records. In summary, the performances of the four methods degrade as the basin size decreases and estimations of IPFs using MDFs for basins larger than 500 km^2 have reasonable accuracy,

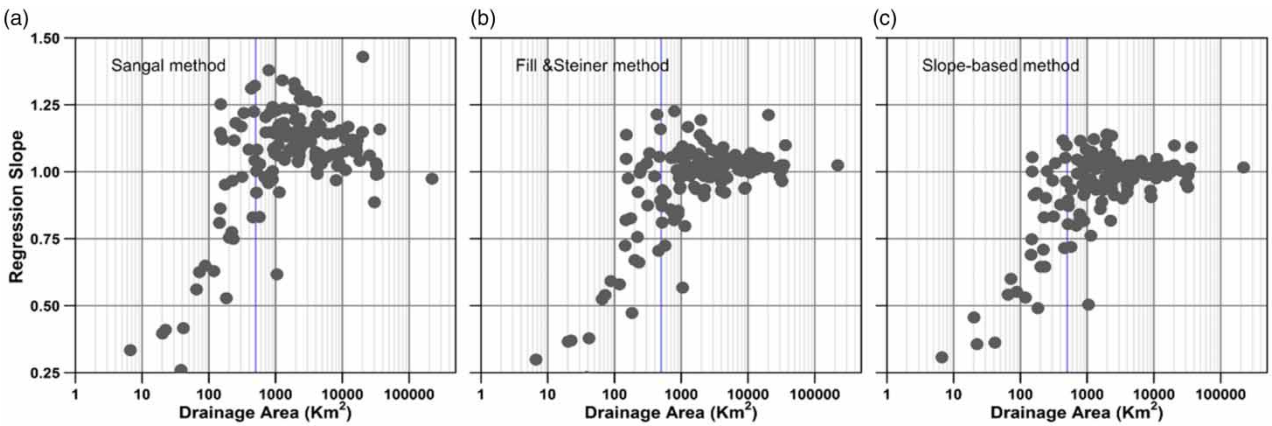

Figure 8 | Basin size dependences of the regression slope of predicted IPFs by (a) Sangal's, (b) Fill and Steiner's and (c) the slope-based methods against observed IPFs.

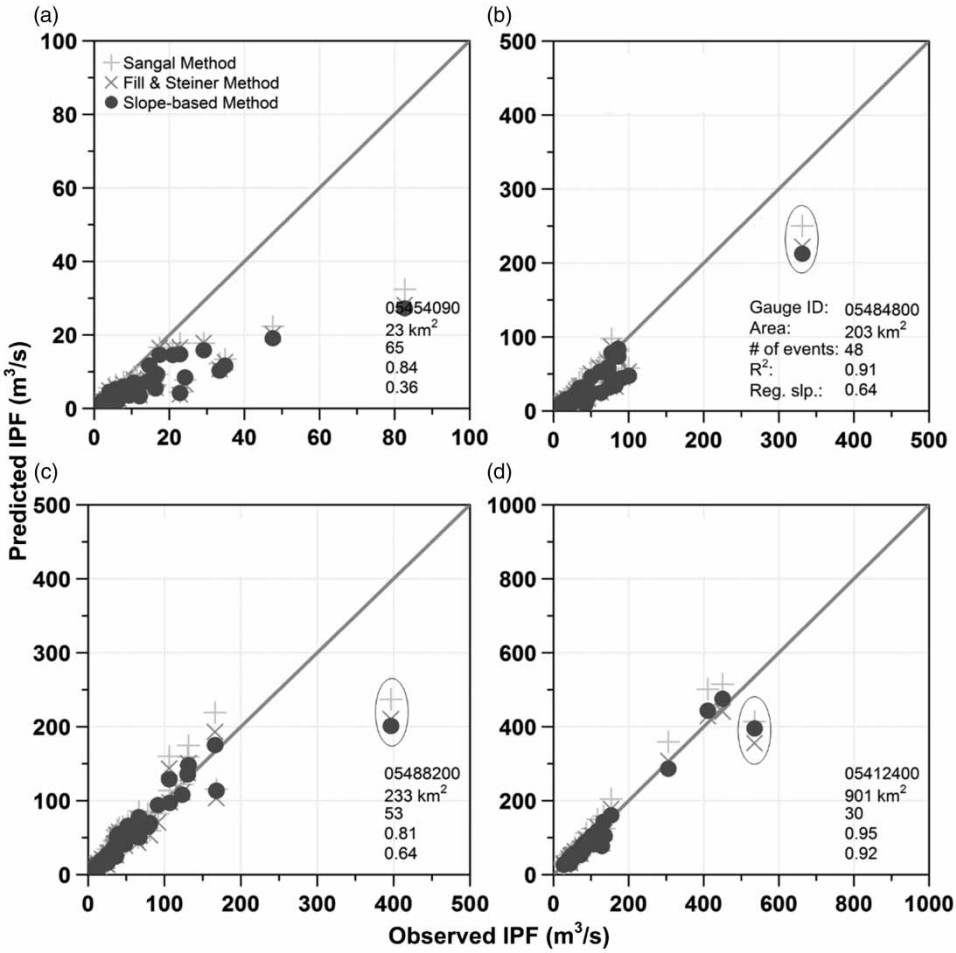

Figure 9 | Limitations of estimating IPFs from MDFs: (a) overall underestimation (i.e., regression slope less than 1) for small basins and (b)-(d) overall underestimation due to one bad prediction (circled dots) resulting from incomplete information available from MDF records.

while the underestimation problem for basins smaller than 500 km^2 deserve further effort. It is interesting to note that, according to Kent's (1973) empirical relationship and assuming a flow velocity of 1 m/s, a basin with a drainage area of 500 km^2 will have a time of concentration of about one day.

CONCLUSION

This study evaluated Fuller's, Sangal's and Fill and Steiner's methods and proposed a slope-based method to estimate IPF from MDF. The new method explicitly adopts the rising and falling slopes to describe the shape of MDF hydrographs and it is simple and requires only MDF records as its input. All four methods were tested at 144 basins in Iowa with drainage areas ranging from 7 to 220,000 km^2. The test involved about 3,800 peak flow events that had different flood generation mechanisms (e.g., rainfall or snow-related events). The application of the four methods in Iowa suggests the following.

Accounting for the dynamics of MDF hydrograph shapes, e.g., by using sequence of MDF rather than just the maximum MDF, is an effective approach to estimate IPFs from MDFs and the four methods are useful. Overall, both in the absolute (MAE) and relative (MAPE and regression slope) senses, Fuller's method has the largest and the slope-based method has the smallest estimation errors of IPFs for basins larger than 500 km^2. Although with large underestimation errors, Sangal's method performs best for basins smaller than 500 km^2.

Fuller's method appears to underestimate, Sangal's method tends to overestimate, Fill and Steiner's method shows good performance and the slope-based method appears to marginally outperform Fill and Steiner's method. For the slope-based method, about 75% of the basins have ±10% prediction error in IPFs (i.e., regression slopes between 0.90 and 1.10) and about 85% of the basins have ±20% prediction error in IPFs (i.e., regression slopes between 0.80 and 1.20).

The performances of the four methods degrade as the basin size decreases. Fill and Steiner's and the slope-based methods work well for basins larger than 500 km^2, work poorly for basins smaller than 100 km^2, and work fairly well for basins with sizes in between; the underestimation problem for basins smaller than 500 km^2 deserves further effort. These two methods generally work well for peak flow events generated from different climatic forcings. Although we recommend further tests if it is feasible, Fill and Steiner's method and the slope-based method are promising tools to use to estimate IPFs from MDFs and further to assist with flood risk management and hydraulic structure design for areas where IPF records are unavailable or insufficient.

ACKNOWLEDGEMENTS

The first author acknowledges the financial support jointly provided by the Project (Grant No. 41501020) and the Foundation for Innovative Research Groups (Grant No. 41321001) of the National Natural Science Foundation of China. The second author acknowledges the support of the Rose & Joseph Summers endowment.

REFERENCES

Canuti, P. & Moisello, U. 1982 Relationship between the yearly maxima of peak and daily discharge for some basins in Tuscany. *Hydrological Sciences Journal* **27**, 111–128.

Criss, R. E. & Winston, W. E. 2008 Do Nash values have value? Discussion and alternate proposals. *Hydrological Processes* **22**, 2723–2725.

Dastorani, M. T., Koochi, J. S., Darani, H. S., Talebi, A. & Rahimian, M. H. 2013 River instantaneous peak flow estimation using daily flow data and machine-learning-based models. *Journal of Hydroinformatics* **15** (4), 1089–1098.

Ding, J., Wallner, M., Müller, H. & Haberlandt, U. 2015 Estimation of instantaneous peak flows from maximum mean daily flows using the HBV hydrological model. *Hydrological Processes*, doi: 10.1002/hyp.10725.

Eash, D. A., Barnes, K. K. & Veilleux, A. G. 2013 *Methods for Estimating Annual Exceedance-Probability Discharges for Streams in Iowa, Based on Data through Water Year 2010.* U.S. Geological Survey Scientific Investigations Report 2013–5086, p. 63 with appendix. http://pubs.usgs.gov/sir/2013/5086/.

Ellis, W. & Gray, M. 1966 Interrelationships between the peak instantaneous and average daily discharges of small prairie streams. *Canadian Agricultural Engineering*, 1–39.

Fill, H. D. & Steiner, A. A. 2003 Estimating instantaneous peak flow from mean daily flow data. *Journal of Hydrologic Engineering* **8**, 365–369.

Fuller, W. E. 1914 Flood flows. *Transactions of the American Society of Civil Engineers* **77**, 564–617.

Gaál, L., Szolgay, J., Kohnová, S., Hlavčová, K., Parajka, J., Viglione, A., Merz, R. & Blöschl, G. 2014 Dependence between flood peaks and volumes: a case study on climate and hydrological controls. *Hydrological Sciences Journal* 1–17, doi: 10.1080/02626667.2014.951361.

Gupta, V. K., Mantilla, R., Troutman, B. M., Dawdy, D. & Krajewski, W. F. 2010 Generalizing a nonlinear geophysical flood theory to medium-sized river networks. *Geophysical Research Letters* **37**, doi: 10.1029/2009gl041540.

Jarvis, C. S. 1936 *Floods in the United States: Magnitude and Frequency*. US Geological Survey.

Kent, K. 1973 A method for estimating volume and rate of runoff in small watersheds. US Department of Agriculture Soil Conservation Service, Washington, DC.

Krause, P., Boyle, D. P. & Bäse, F. 2005 Comparison of different efficiency criteria for hydrological model assessment. *Adv. Geosci.* **5**, 89–97.

Langbein, W. 1944 Peak discharge from daily records. *Water Resources Bulletin* **145**.

Legates, D. R. & McCabe, G. J. 1999 Evaluating the use of 'goodness-of-fit' measures in hydrologic and hydroclimatic model validation. *Water Resources Research* **35**, 233–241.

Piñeiro, G., Perelman, S., Guerschman, J. P. & Paruelo, J. M. 2008 How to evaluate models: observed vs. predicted or predicted vs. observed? *Ecological Modelling* **216**, 316–322.

Prior, J. C. 1991 *Landforms of Iowa*. University of Iowa Press, Iowa City, IA.

Sangal, B. P. 1983 Practical method of estimating peak flow. *Journal of Hydraulic Engineering* **109**, 549–563.

Schaefli, B. & Gupta, H. V. 2007 Do Nash values have value? *Hydrological Processes* **21**, 2075–2080.

Serinaldi, F. & Kilsby, C. G. 2013 The intrinsic dependence structure of peak, volume, duration, and average intensity of hyetographs and hydrographs. *Water Resources Research* **49**, 3423–3442.

Taguas, E. V., Ayuso, J. L., Pena, A., Yuan, Y., Sanchez, M. C., Giraldez, J. V. & Pérez, R. 2008 Testing the relationship between instantaneous peak flow and mean daily flow in a Mediterranean Area Southeast Spain. *CATENA* **75**, 129–137, doi: http://dx.doi.org/10.1016/j.catena.2008.04.015.

Tan, K.-S., Chiew, F. H. S. & Grayson, R. B. 2007 A steepness index unit volume flood hydrograph approach for sub-daily flow disaggregation. *Hydrological Processes* **21**, 2807–2816.

Willmott, C. J. & Matsuura, K. 2005 Advantages of the mean absolute error (MAE) over the root mean square error (RMSE) in assessing average model performance. *Climate Research* **30**, 79–82.

Willmott, C. J. & Matsuura, K. 2006 On the use of dimensioned measures of error to evaluate the performance of spatial interpolators. *International Journal of Geographical Information Science* **20**, 89–102.

First received 19 July 2016; accepted in revised form 9 December 2016. Available online 20 March 2017